$$I_{Cu} = I_{Cu}^{Max} \exp(-\frac{\ell}{d_0}) \qquad (1)$$

where I_{Cu}^{Max} = intensity of a clean copper Auger peak; d_o = mean free path of copper Auger electrons at 920 eV in the iron film and ℓ = pathlength traversed by the detected electrons. ℓ is related to the thickness of the iron overlayer, d_{Fe}, by $\ell \cos\theta = d_{Fe}$, where θ is the CMA acceptance angle (42.3°) relative to the surface normal. In Figure 2, we have also plotted the theoretical curve for the decrease in the intensity of the substrate Auger peak with deposition time. Here we took d_{Fe} = kt, where t = deposition time and k = proportionality constant. k was determined by plotting $\ln \frac{I_{Cu}}{I_{Cu}^{Max}}$ versus deposition time. The agreement between the theoretical and experimental curves suggests that iron grows approximately layer-by-layer on Cu(100) in spite of the absence of well defined linear segments observed in some cases of layer-by-layer growth [2,3].

The iron coverage in this study was estimated by the attenuation of the 920 eV copper Auger peak with iron deposition according to Equation (1).

The Auger spectra between 30 and 130 eV for various iron coverages are shown in Figure 3. The copper $M_{2,3}VV$ and the M_1VV Auger transitions are observed to decrease in intensity with iron deposition.

3.2. LEED Patterns

With a few layers of iron deposited on Cu(100), a clear (1X1) LEED pattern was observed (Figure 4a). For higher iron coverages, faint half order (±1/2, ±1/2) spots appeared (Figure 4b), probably due to a slight amount of oxygen contamination.

The (1X1) LEED pattern observed for low coverage of iron deposited on Cu(100) is indicative of epitaxial growth of iron on Cu(100) to form f.c.c. iron in agreement with previous works [4,5].

Using the graphite instead of the alumina boat for iron deposition, a p(2X2) LEED pattern was observed when more than two layers of iron were deposited (Figure 4c). The p(2X2) structure could be due to carbon contamination since Auger spectroscopy showed that there was more carbon in the deposited iron together with a small amount of oxygen. Heating the surface with deposited iron to 500°C resulted in the disappearance of both carbon and oxygen Auger signals and loss of the p(2X2) pattern. The iron Auger intensities were observed to decrease due to diffusion of iron into the bulk or evaporation from the surface. After this surface was heated with $2X10^{-8}$ torr of C_2H_4 for 5 min, carbon deposition was observed with Auger spectroscopy and the p(2X2) LEED pattern reappeared. This shows that the p(2X2) structure is due to carbon contamination.

Compared with a previous LEED measurement of iron or Ni(100) [6] we note that a relatively thicker layer of f.c.c. iron can be formed on Cu(100). This is due to the fact that γ-iron has a lattice constant (3.588 Å at room temperature [7]) closer to that of bulk copper (3.61 Å) than that of bulk nickel (3.52 Å).

Figure 4d shows the LEED pattern for a thick layer of iron on Cu(100) (the copper Auger peaks were not observed with Auger spectroscopy). The half-order spots are due to contamination. At such high iron coverages, b.c.c. iron formation has been observed [4] although in the LEED patterns we cannot distinguish b.c.c. (100) iron from f.c.c. iron (both have four-fold symmetry).

3.3. EELS Measurements

Auger spectroscopy showed a small amount of carbon and oxygen contaminants in the deposited iron. However, the EEL spectra obtained for the Cu(100) surface with an iron overlayer after heating to 500°C (to eliminate carbon and oxygen) did not show any observable differences from those taken in in the presence of a small amount of carbon and oxygen. Thus, we do not attribute the electron energy loss features to carbon or oxygen contaminants.

3.3.1. **Clean Cu(100)** - The electron energy loss spectra of clean Cu(100) obtained with E_p = 50, 150 and 300 eV are shown in Figure 5. The energy losses labeled a to k are listed in Table 1. They are compared with those obtained for Cu(100), (111), (311), polycrystalline copper and evaporated copper films obtained by other investigators [8-17]. The assignments of the loss peaks by various authors are indicated.

Peak a has been observed in all previous studies. It has been invariably described as an interband transition from the copper d-band to empty states above the Fermi level [8,9,11-13,15]. Peak b has been ascribed as a volume plasmon [9-11], a surface plasmon [8,12,13,15] or an interband transition [12]. Peak c has been attributed to an interband transition in agreement with theoretical calculations [18,19]. Peak d was observed by Jenkins et al. [14] for a Cu(111) crystal and by Montano et al. [17] for a thick copper film on Ni(100). No assignment for this peak has been made. Peak e has been shown to be a volume plasmon after Powell's investigation [20] of the Al-Cu alloy films for various concentrations of aluminum and copper. The loss energy was observed to shift continuously from 20 eV in pure copper to 15 eV in pure aluminum. The continuous shift in loss energy was explained by the change in electron density which participates in the plasma oscillations as the aluminum concentration was increased. At E_p = 50eV, Fig. 4 shows that peak e is relatively weak and it appears that it has shifted to 23.9eV. This can be due to the disappearance of the volume plasmon peak at 20eV but the contribution from an interband transition remains at 23.9eV. The assignment of peak e partially or entirely to an interband transition has been made previously [8,10,12,13,16]. Peak f has been identified as an interband transition [9-

13,16] or multiple losses [12,13]. The observation that this peak is quite strong even at E_p = 50eV supports the assignment that peak f is an interband transition. Peaks g, h and i are not visible in our spectra. The weak peaks j and k obtained with E_p = 300 eV are due to Cu $M_{2,3}$ ionization. Peaks ℓ and m are the $M_{2,3}VV$ copper Auger transitions.

3.3.2. Low Iron Coverage ($\Theta \leq 4$ ML) - The changes in the EEL spectra obtained with E_p = 150 eV for less than 4 ML Fe are shown in Figure 6. At these coverages, the electron energy loss peaks of the Cu(100) substrate are distinguishable although there may be diminution in intensities and/or changes in peak widths. With iron deposition, there is a large decrease in the intensity of peak a. Peaks b and c are also observed to decrease in amplitude but to a smaller extent. Peak d appears as a shoulder in clean Cu(100) and remains with a small amount of iron deposited indicating that it is not a surface plasmon. Since a peak of about the same energy is observed at high iron coverages, this peak can also be attributed to the iron overlayer. Peaks e and f decrease in intensity and broaden. At 3.3 ML Fe, peak c appears to increase in intensity and shifts to lower energy. This is due to the emergence of a loss peak of the iron film with loss energy of about 8 eV. At this coverage, peak f is relatively weak and has lower loss energy.

The electron energy loss features observed with E_p = 150 eV are due to the Cu(100) substrate as well as the iron overlayer since at these coverages the copper $M_{2,3}VV$ Auger peaks are present in the EEL spectra. The decrease in intensity of peak a with iron coverage is in qualitative agreement with the interpretation that this peak is due to a transition from the Cu 3d band to empty states above the Fermi level. The decrease in intensity is due partly to the perturbation of the Cu 3d band and partly to the change in the density of empty states involved in the transitions in the presence of adsorbed iron atoms.

At 1.2 ML Fe, peak b remains relatively strong with no shift in loss energy. This observation does not support the interpretation that this peak is a surface plasmon [8,12,13,15].

Figure 6 shows the changes in the Fe 3p ionization loss with iron coverage. This loss appears as a doublet due to the Fe $3p_{3/2}$ and Fe $3p_{1/2}$ levels produced by spin-orbit splitting. There is a downward shift in energies (about 0.5 eV) for a few iron layers. This is attributed to the change in the density of states of the d-band in the presence of iron.

3.3.3. High Iron Coverage ($\Theta > 4$ ML) - At greater than 4 ML Fe, new features appear in the EEL spectra as shown in Figure 7. Peaks at 3.0 (peak 1), 4.3 (peak 2), and 8.4 (peak 3) eV are interpreted as interband transitions of the f.c.c. iron film produced by the epitaxial growth of iron on Cu(100). The peaks at 16.5 and 23.5 eV correspond to energy losses that appear in α-iron. The peaks at 18.8 and 26.1 eV appear to correspond to peaks e and f of Cu(100). Since they remain at relatively high iron coverages (greater than 7ML), they must come from the iron overlayer. The energy losses at 16.5 and 23.5 eV have been shown to be due to volume plasmons of α-iron [6]. One may c conjecture that the energy losses at 18.8 and 26.1 eV are due to the volume plasmons of the f.c.c. iron layer, since f.c.c. iron has a higher density (8.03 gm/c.c. at room temperature) than α-iron (7.87 gm/c.c.) and it is known that volume plasmon energy increases with the density of the electrons involved in the oscillations. If this is true, we would expect that there would be a continuous shift in volume plasmon energies from those of f.c.c. iron to those of b.c.c. iron as the average electron density involved in the plasmon oscillations changes with the appearance of b.c.c. iron. The absence of any evidence of energy shifts does not support the interpretation that the peaks at 18.8 and 26.1 eV are volume plasmons of the f.c.c. iron film. Moreover, if one associates the peaks at 16.5 and 23.5 eV with b.c.c. iron, our EEL spectra would suggest that b.c.c. iron should appear at about 4 ML (~7 Å) Fe, but no b.c.c. iron has been observed using electron diffraction for 20 Å of iron on Cu(100) [4]. Hence, we associate the energy losses at 16.5, 18.8, 23.5, and 26.1 eV with the f.c.c. iron film.

With continued deposition of iron, the peak at 5 eV decreases in intensity and the peaks at 19 and 26 eV are gradually replaced by peaks at 16.3 and 23.3 eV of the thick iron film. The EEL spectrum of the thick iron film resembles that of α-iron reported previously [6]. We note the appearance of the intense peak at 5 eV and the weaker peak at 8.4 eV attributed to interband transitions from the Fe 3d band of α-iron to empty states above the Fermi level.

The energy losses for various iron coverages are summarized in Table 2.

4. CONCLUSIONS

We have studied the growth of iron on Cu(100) using Auger spectroscopy, LEED and Electron Energy Loss Spectroscopy. The LEED pattern showed that iron grows epitaxially in an approximately layer-by-layer fashion on Cu(100) to form f.c.c. iron. The existence of the LEED pattern to a thick layer of iron on Cu(100) suggests that iron grows in an orderly by fashion for all iron coverages although the we cannot distinguish between f.c.c. iron and b.c.c. iron in the LEED patterns. EELS measurements showed changes in the electronic structure from that of bulk copper to that of bulk iron. Energy losses at 3.0, 4.3, and 8.1 eV are attributed to interband transition sof the f.c.c. iron film. We also associate the energy losses at 16.5, 18.8, 23.5, and 26.1

eV with the f.c.c. iron overlayer. For a thick iron film on Cu(100), the spectrum resembles that of α-iron.

Acknowledgment: This work was supported by the U.S. Department of Energy.

REFERENCES

1. M.P. Seah, Surf. Sci. 32(1972)703.
2. C. Binns and C. Norris, Surf. Sci. 115(1982)395.
3. B.C. DeCooman, V.D. Vankar and R.W. Vook, Surf. Sci. 128(1983)128.
4. W.A. Jesser and J.W. Matthews, Phil. Mag. 15(1967)1097.
5. W. Wiartolla, W. Becker, W. Keune and H.D. Pfannes, J. Phys. 45(C5)(1984)461.
6. Y.C. Lee, M. Abu-Joudeh and P.A. Montano, Surf. Sci. 143(1984)469.
7. W. Keune, R. Halbauer, U. Gonser, J. Lauer and D.L. Williamson, J. Appl. Phys. 48 (7) (1977) 2976.
8. J.L. Robins and J.B. Swan, Proc. Phys. Soc. 76(1960)857.
9. D.L. Misell and A.J. Atkins, Phil. Mag. 27(1973)95.
10. E.J. Scheibner and L.N. Tharp, Surf. Sci. 8(1967)247.
11. I. Marklund, S. Andersson and J. Martinson, Arkiv Fysik 37(1968)127.
12. L.K. Jordan and E.T. Scheibner, Surf. Sci. 10(1968)373.
13. A.R.L. Moss and B.H. Blott, Surf. Sci. 17 (1969)240.
14. L.H. Jenkins and M.F. Chung, Surf. Sci. 63(1977)182.
15. H. Papp, Surf. Sci. 63(1977)182.
16. C. Benndorf, B. Egert, G. Keller and F. Thieme, Surf. Sci. 74(1978)216.
17. P.A. Montano, P.P. Vaishnava and E. Boling, Surf. Sci. 130(1983)191.
18. B. Segall, Phys. Rev. 125(1962)109.
19. A. Ia. Viatskin, J. Techn. Phys. (USSR) 3(1958)2038,2252.
20. C.J. Powell, Australian J. Phys. 13(1960)145.

TABLE 1. Electron Energy Losses of Clean Copper (eV)

	E_p(eV)	a	b	c	d	e	f	g	h	i	j	k		Reference
(100)	50 (r)	3.7	7.2	10.1	17.4	23.9	28.2	-	-	-	-	-	-	This work
"	150 (r)	4.3	7.3	10.1	16.7	19.7	27.0	-	-	-	-	-	-	" "
"	300 (r)	5.1	7.5	-	-	19.1	27.8	-	-	-	78.1		80.7	" "
Evaporated Film	1200 (r)	$4.5^{(1)}$	$7.6^{(2)}$	-	-	$19.1^{(1,3)}$	$27.3^{(1,4)}$	-	-	-	-	$77.4^{(5)}$		[8]
Evaporated Film	$60,000^{(t)}$	$4.6^{(1)}$	$8.5^{(3)}$	$11.9^{(1)}$	-	$19.3^{(3)}$	$27.2^{(1)}$	-	-	-	-	-		[9]
(100)	190 (r)	4.0	$9.2^{(3)}$	-	-	$20.5^{(1)}$	$28^{(1)}$	-	-	-	-	-		[10]
(111)	60-140(r)	$4.3^{(1)}$	$7.6^{(3)}$	$10.1^{(1)}$	-	19.0	$27.2^{(1)}$	-	-	-	-	$74^{(5)}$		[11]
(100), (111)	30-350(r)	$4.5^{(1)}$	$7.5^{(1,2)}$	-	-	$19.5^{(1,3)}$	$27.5^{(1,4)}$	$39.0^{(4)}$	-	-	-	-		[12]
Evaporated Film	300 (r)	$4.4^{(1)}$	$7.6^{(2)}$	-	-	$19.5^{(1,3)}$	$28.5^{(1,4)}$	$40^{(4)}$	$50^{(1,4)}$	$69^{(1)}$	-	-		[13]
(111)	190.5 (t)	4.0	7.4	11.8	17.0	19.0	26.6	37.0	46.8	58	-	-		[14]
(311)	150 (t)	$4.5^{(1)}$	$7.7^{(2)}$	$10.5^{?}$	-	$19.0^{?}$	27.5	$39^{(4)}$	$48^{(4)}$	-	-	-		[15]
(100)	400 (t)	3.9	7.1	9.7	-	$18.8^{(1)}$	$26.5^{(1)}$	-	-	$59^{?}$	-	$74.5^{(5)}$		[16]
Evaporated Film	300 (r) 150 (r)	4 3.8	7 7	10 10	16 16	19 19	27 27	35 -	46 -	58 -		75 -		[17]

TABLE 2. Electron Energy Losses of Cu(100) for Various Iron Coverages (eV).
(E_p = 150 eV)

(a) Low iron coverages

Fe (ML)	a	b	c	d	e	f
0	4.3	7.3	10.1	16.7	19.7	27.0
1.2	3.8	7.5	10.0	16.7	19.3	27.2
2.2	3.9	7.5	9.4	15.8	19.4	27.1
3.3	3.9	7.5	9.3	15.5	19.5	26.7

(b) High iron coverage

Fe (ML)	1	2	3	4	5	6	7
7	3.0	4.3	8.1	16.5	18.8	23.5	26.1
11	-	4.5	7.9	16.4	19.0	23.7	26.3
25	-	5.1	7.9	17.8	-	25.5	25.5
thick iron overlayer		5.0	8.4	16.3	-	23.3	-

FIGURE CAPTIONS

FIGURE 1 Auger spectra for Cu(100) for various iron coverages: (a) 0 ML; (b) 0.3 ML; and (c) 1.6 ML.

FIGURE 2 Variation of the intensities of the 920 eV copper Auger peak and the 651 eV iron Auger peak versus deposition time. The theoretical curve for diminution of the intensity of the copper Auger signal for a layer-by-layer growth is also shown.

FIGURE 3 Low energy Auger spectra (0 to 130 eV) of Cu(100) for various iron coverages: (a) 0 ML; (b) 1 ML; (c) 2 ML; and (d) 4 ML.

FIGURE 4 LEED Patterns for Fe on Cu(100):(a) 4.2 ML (E_p = 113 eV), (b) 8 ML (E_p = 125 eV), (c) 5 ML (E_p = 119 eV) and (d) Thick iron layer (E_p = 123 eV).

FIGURE 5 EEL spectra of clean Cu(100): (a) E_p=300 eV, (b) E_p=150 eV, and (c) E_p=50 eV.

FIGURE 6 EEL spectra of Cu(100) deposited with (a) 1.2 ML, (b) 2.2 ML and 3.3 ML Fe (E_p=150 eV).

FIGURE 7 Fe 3p ionization at (a) 1.2 ML, (b) 2.2 ML, and (c) 3.3 ML Fe (E_p = 150 eV).

FIGURE 8 EEL spectra of Cu(100) deposited with (a) 7 ML, (b) 11 ML, (c) 25 ML iron, and (d) thick iron layer (E_p=150 eV).

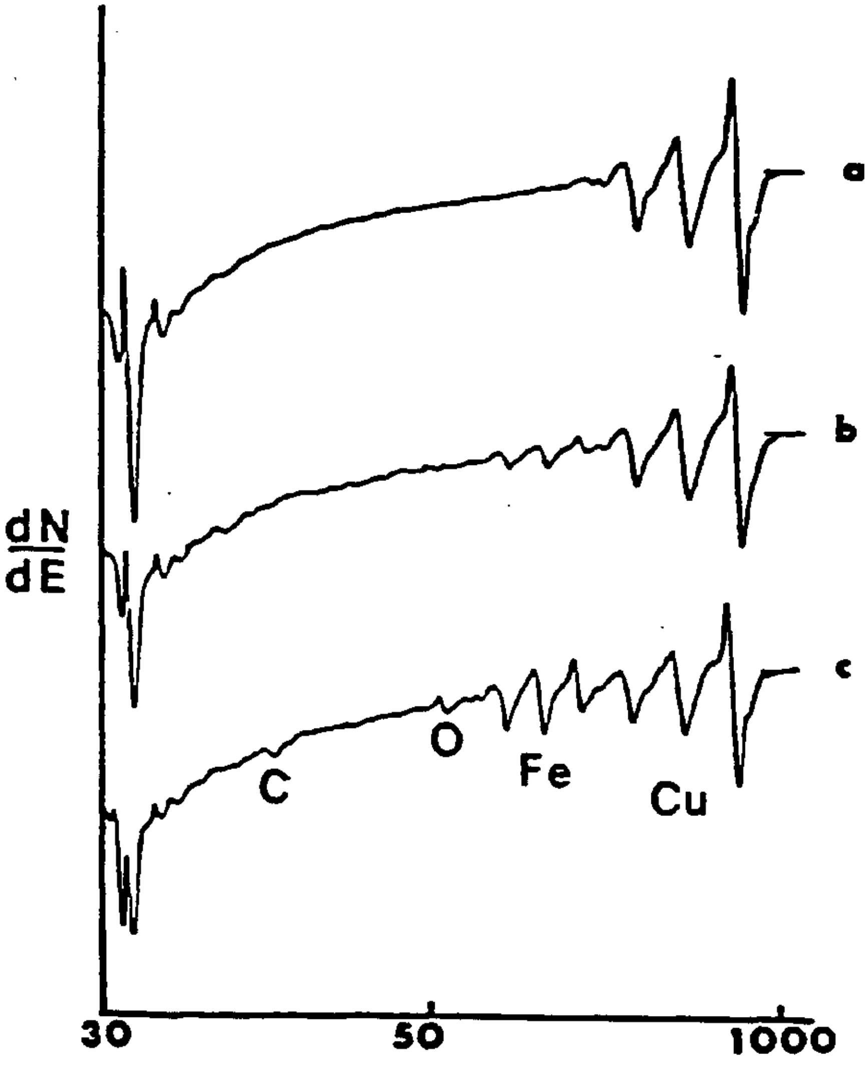
dN/dE
a
b
c
C
O
Fe
Cu
30
50
1000
Electron Energy (eV)

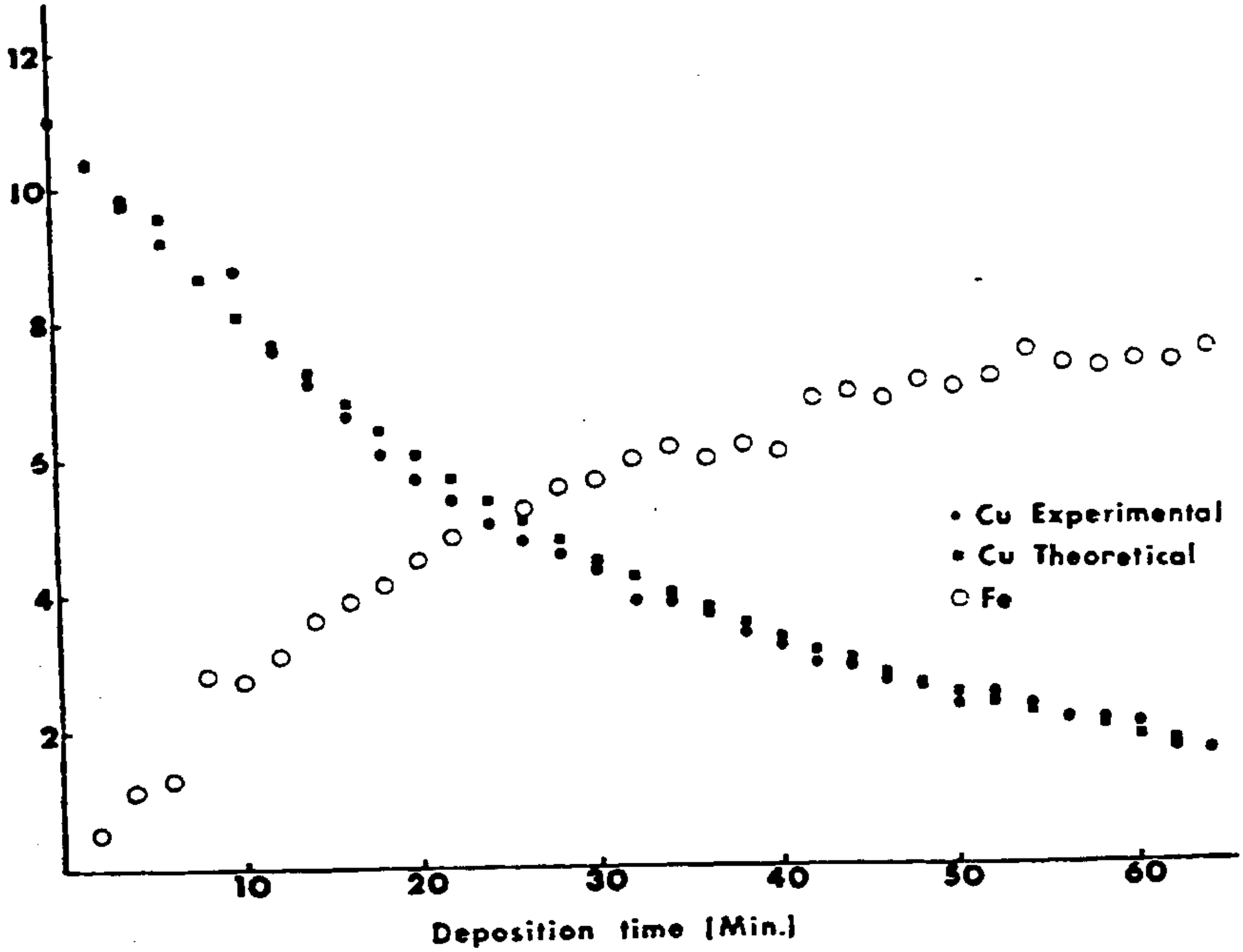
12
10
8
6
4
2
10
20
30
40
50
60
Deposition time (Min.)
• Cu Experimental
▪ Cu Theoretical
○ Fe

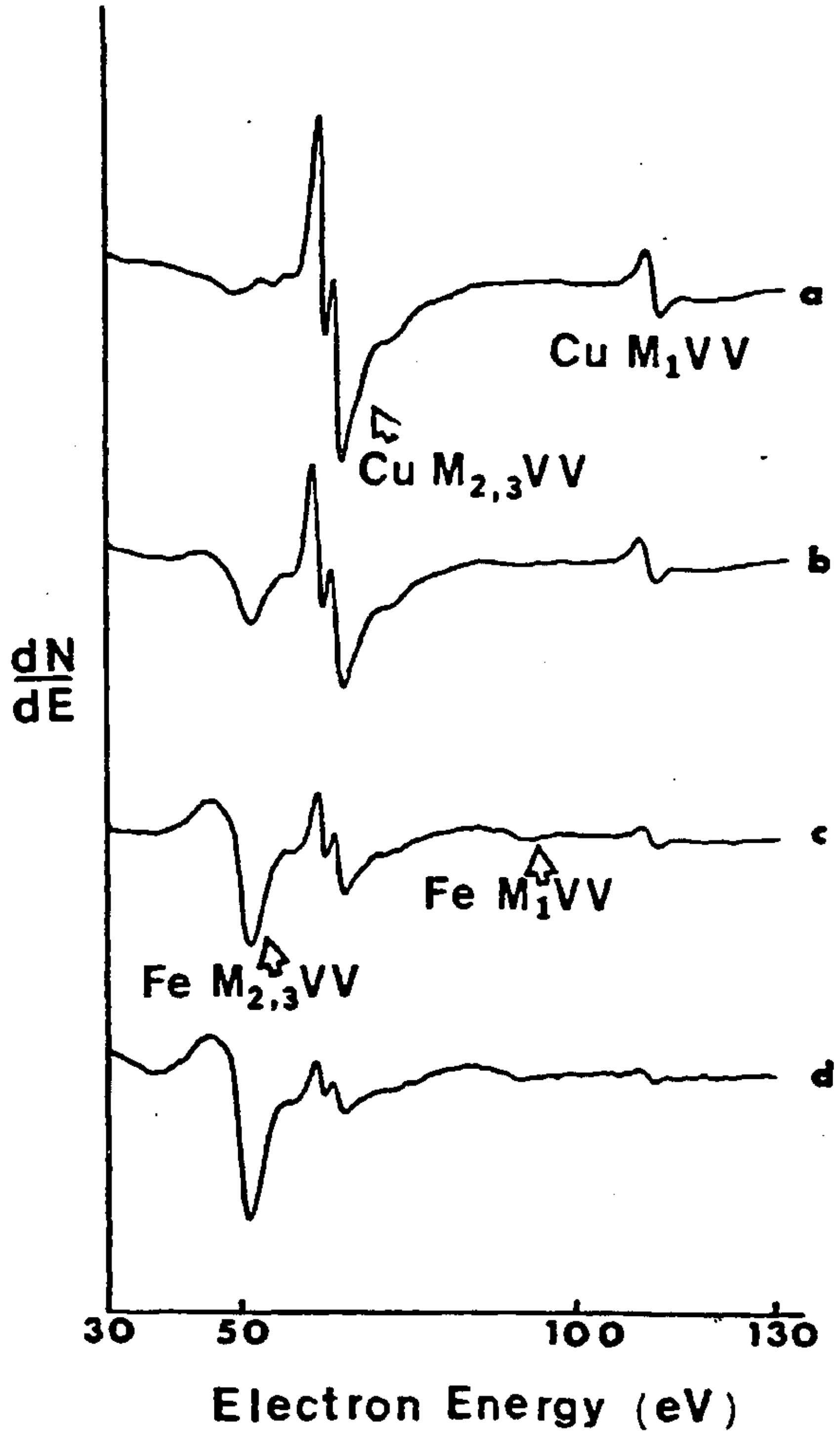
Cu M_1VV
Cu $M_{2,3}VV$
Fe M_1VV
Fe $M_{2,3}VV$
a
b
c
d
dN/dE
30
50
100
130
Electron Energy (eV)

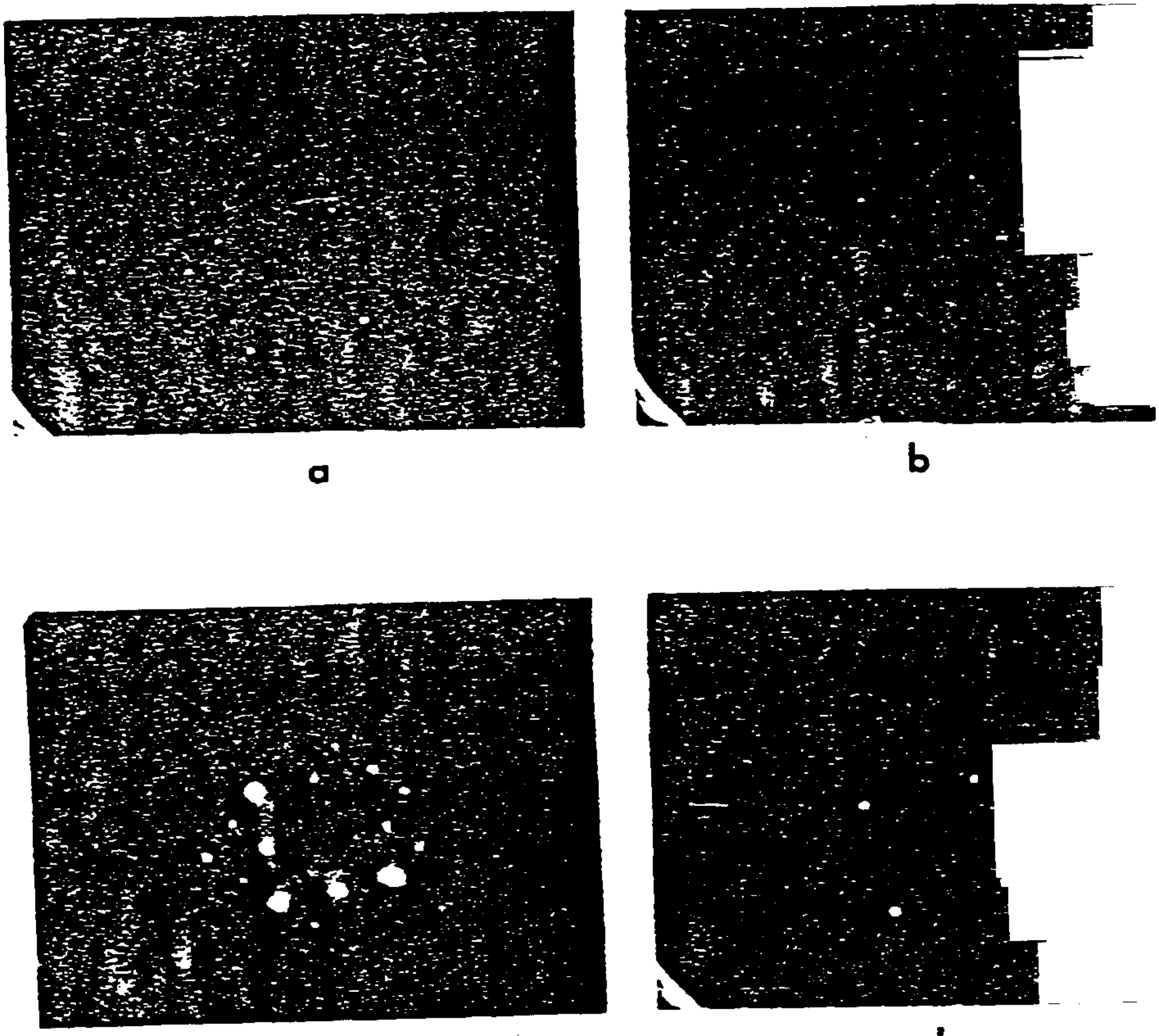
a
b
c
d

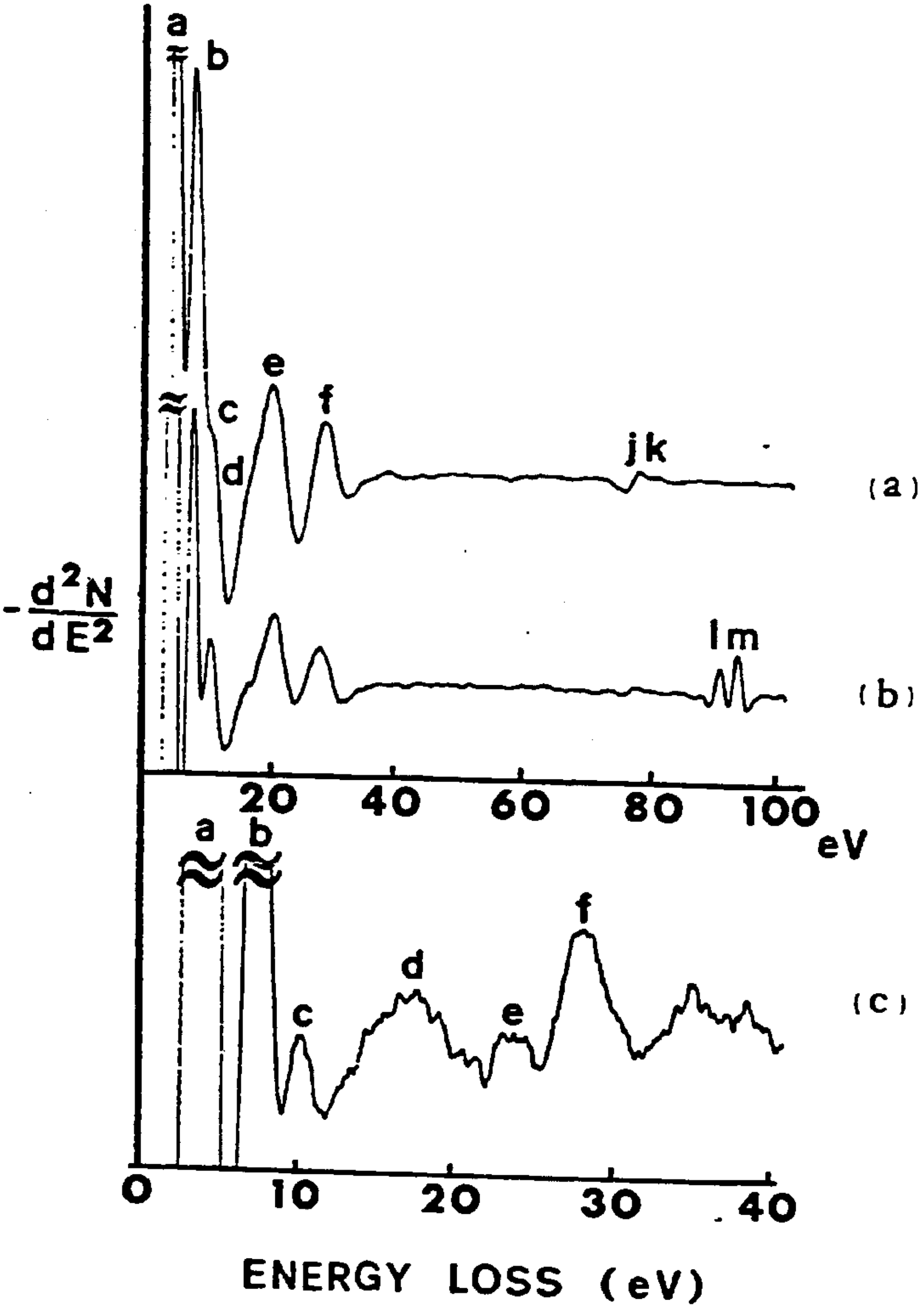
a
b
c
d
e
f
jk
lm
(a)
(b)
(c)
$-\frac{d^2N}{dE^2}$
20
40
60
80
100
eV
a
b
c
d
e
f
0
10
20
30
40
ENERGY LOSS (eV)

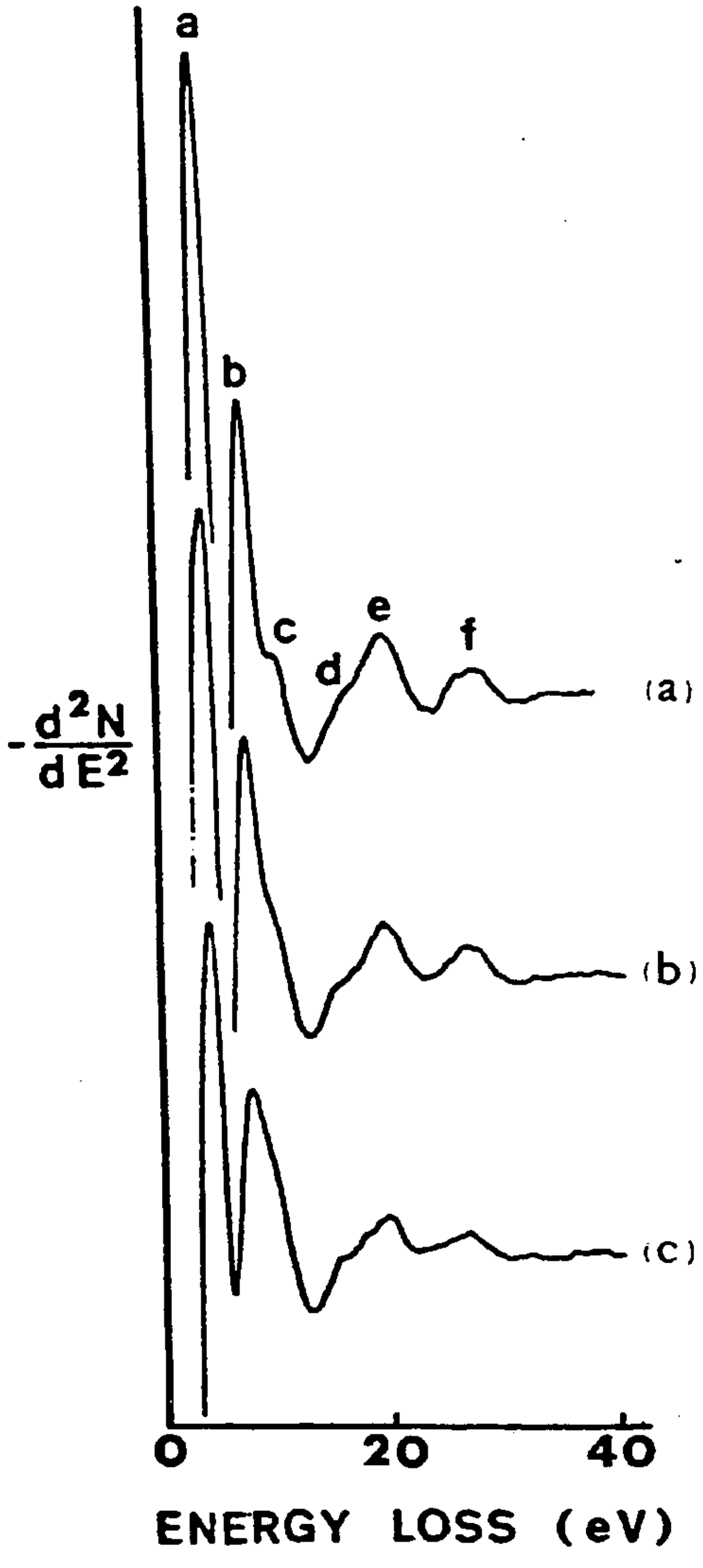
a
b
c
d
e
f
(a)
(b)
(c)
$-\frac{d^2N}{dE^2}$
0
20
40
ENERGY LOSS (eV)

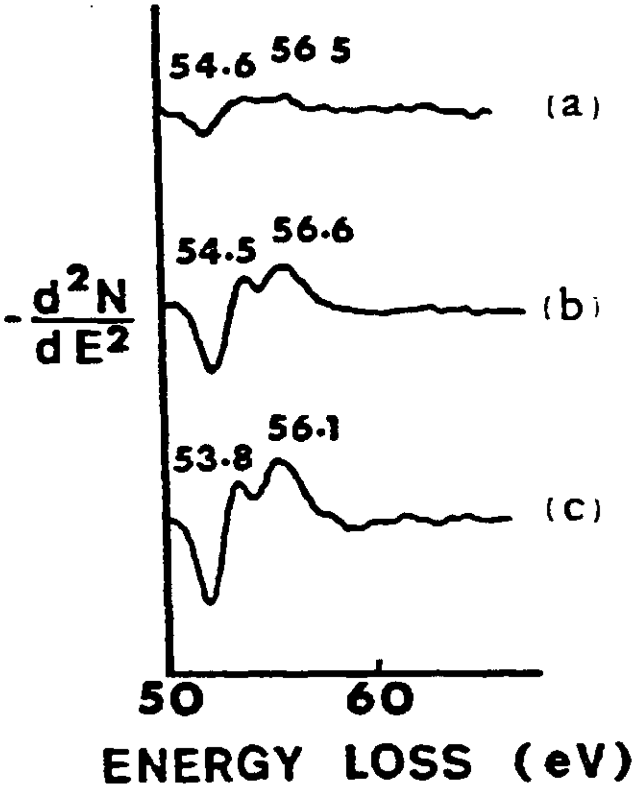
54.6
56 5
(a)
54.5
56.6
(b)
53.8
56.1
(c)
$-\frac{d^2N}{dE^2}$
50
60
ENERGY LOSS (eV)

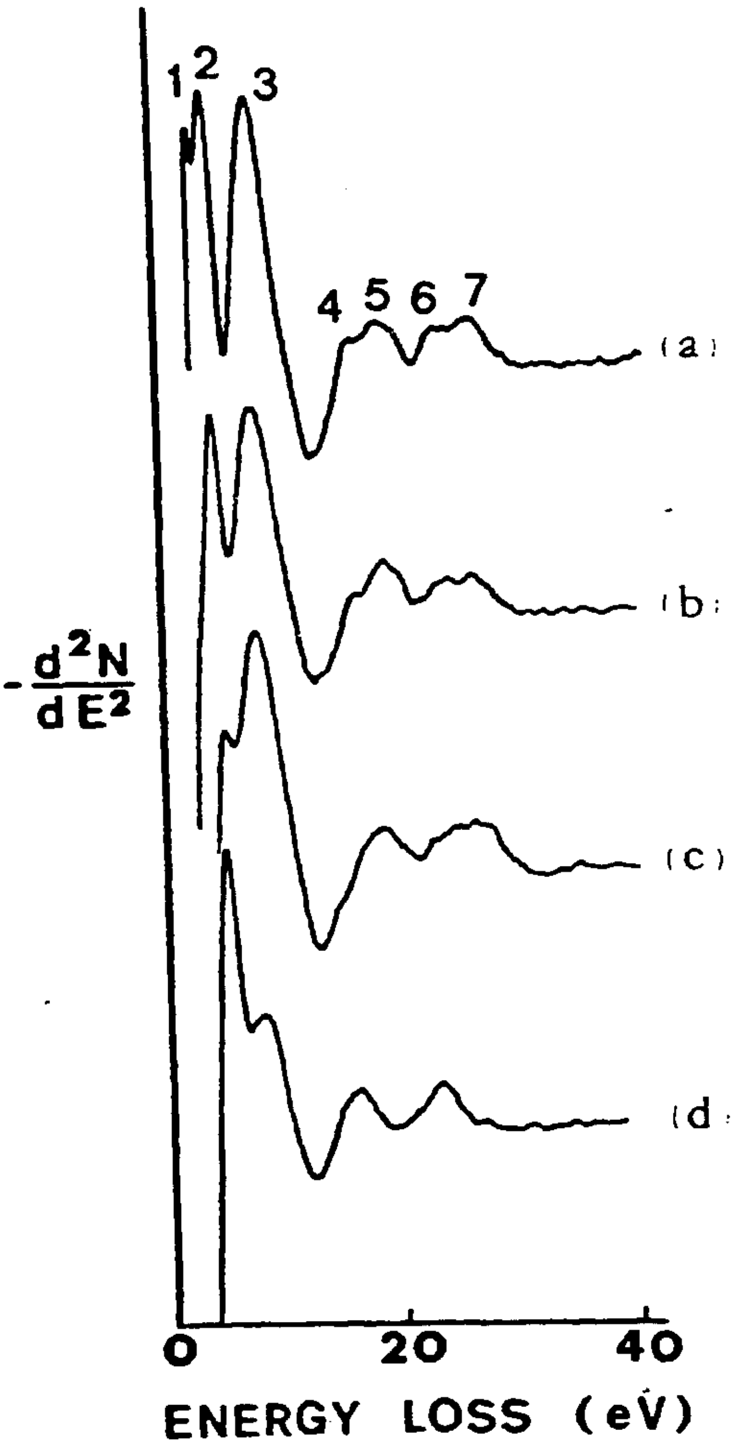
1
2
3
4
5
6
7
(a)
(b)
(c)
(d)
$-\frac{d^2N}{dE^2}$
0
20
40
ENERGY LOSS (eV)

7. LEED MEASUREMENTS OF ONE MONOLAYER OF IRON ON Cu(111)

(Quarterly REport April 16, 1987 - July 15, 1987)